SATURATED FINITE-TIME SLIDING MODE CONTROL FOR EXOSKELETON ROBOT

Ratiba Fellag [1] [2], Mohamed Guiatni [3], Mustapha Hamerlain [1], Noura Achour [2]

In this work, a saturated third-order sliding mode controller is designed for motion tracking regulation of a five degrees-of-freedom exoskeleton robot utilized in physiotherapy rehabilitation of upper limbs. This robot helps to assist the movements of patients with motor disabilities. The challenge is to design an adequate control system to achieve smooth trajectory tracking with good precision regardless of uncertainties and disturbances. Consequently, it is developed, in this work, a new saturated homogeneous sliding mode law based on third order super twisting algorithm featuring finite-time convergence. The controller keeps the essential robustness characteristics of sliding modes. And further takes into account the saturation of electric actuators. This boundedness property allows to obtain better performances and to extend life-time of actuators. To illustrate benefits of the elaborated saturated control it is compared to unsaturated controller through simulations of passive rehabilitation exercises.

Keywords: Saturation , Robustness , Higher order sliding modes , exoskeleton rehabilitation robot

1. Introduction

Eating, personal care and handling items are some daily life activities requiring motion of human upper limb extremities. These movements, that are insignificant for healthy individuals, become a burden for those who are disabled. The number of people living with disabilities across the world is increasing, mainly due to neurological disorders such as stroke. A number of robotic devices, also known as exoskeletons, have been created for upper limb recovery [1, 2] apart from traditional rehabilitation, which is performed by manual exercises by physiotherapists. These robotic devices provide intensive, repetitive, reliable, and personalized care while maintaining patient safety and reducing therapist workload.

[1] Robotic and Industrial Automation Laboratory (DPR), Centre de Développement des Technologies Avancées, Algiers, Algeria e-mail: rfellag@cdta.dz , mhamerlain@cdta.dz

[2] Robotics Parallelism and Electro-energetic Laboratory (LRPE), Université des Sciences et de la Technologie Houari Boumediene, Algiers, Algeria noura.achour@gmail.com

[3] Complex System Control and Simulators Laboratory (LCS^2), Ecole Militaire Polytechnique, Algiers, Algeria e-mail: mohamed.guiatni@gmail.com

Exoskeleton robots have rigid external structures with actuators that allow for coordinated and precise movements, as well as sensors that provide information on movement such as angle, speed, and acceleration. These devices are attached to the upper limb at multiple points and are controlled as to achieve the best performance in trajectory tracking of rehabilitation exercises movements. The main goal is to allow for healthy movement with minimal resistance. Patients may either actively be engaged in the training activities or be passive to the robot [3] depending on the rehabilitation mode.

Several control methodologies including both linear and nonlinear approaches have been applied to exoskeleton rehabilitation robots [4]. This work is focused in nonlinear robust sliding mode control [5]. Well reputed for its robustness, various sliding mode approaches have been implemented on upper limb exoskeleton robots involving classic sliding control in [6, 7], a nonsingular terminal sliding mode in [8, 9], adaptive sliding modes in [10, 11], adaptive integral sliding mode control [12, 13]. However, these controllers do not fully take into account the physical constraints posed by the actuators.In practice, the control input's limitations, which typically take the form of a saturation function, must be taken into account. In order to address these limitations, additional modifications are required to the control laws.

The main contribution of this work is to propose a saturated finite-time third order sliding mode controller which extends the super-twisting algorithm. To the best knowledge of the authors, no other work in the literature has proposed a saturated third-order STA control approach. The most recent works proposing saturated second order sliding mode controllers are summarized in [14]. This research includes a relay controller based on Lyapunov-level curves allowing the algorithms to generate bounded control signals. Other versions of saturated super-twisting are formulated in [15–17]. They generate a bounded control signal while compensating for bounded Lipschitz uncertainties/perturbations with a finite-time convergence. Besides, in [18], authors elaborated a saturated continuous twisting algorithm.

Motivated by the above-mentioned controllers, and based on third order algorithm (3-STA) [19], a saturation function is introduced to adjust the input control generated by the controller as to respect the physical constraints of the actuators of the exoskeleton robot. The design procedure is simpler, and the elaborated controller generates a continuous control signal that prevents chattering while preserving inherent robustness of sliding modes. It guarantees as well a fast and accurate finite-time convergence to the desired position profile under parameter uncertainties and disturbances.

To demonstrate the efficiency of the proposed control strategy, simulations of trajectory tracking are achieved on the upper limb exoskeleton robot presented in [11]. This adopted device has been exploited in recent works proposing new control strategies [20–22]. Its dynamic model is convenient

for simulations since it is nonlinear, coupled and uncertain characterizing five degrees-of-freedom. Furthermore, it is complete. Information about inertial and gravitational constants as well as motor specifications are available in [11, 23, 24]. These details permit the simulations tests to be closer to real conditions.

The remainder of this work is divided into the following sections. The problem statement is described in section 2, followed by a description of the exoskeleton system and its dynamic model. The design methodology for the saturated controller is examined in section 3. Whereas, in section 4, the simulation results are drawn and evaluated. Lastly, section 5 concludes the work.

2. Problem Statement

It is presented, in this section, the five-degrees-of-freedom exoskeleton robot that will be exploited throughout this work as well as its dynamic model.

2.1. Description of the system

The exoskeleton robot under investigation is the one seen in [11, 25]. Figure. 1 depicts the device. The actual structure ,shown in Figure. 1a, is made up of five degrees of freedom and mimics human upper extremity movements. An electrical servomotor is used at each joint of the exoskeleton robot to provide the required power to the arm. Each joint's absolute position is recorded using optical encoders.

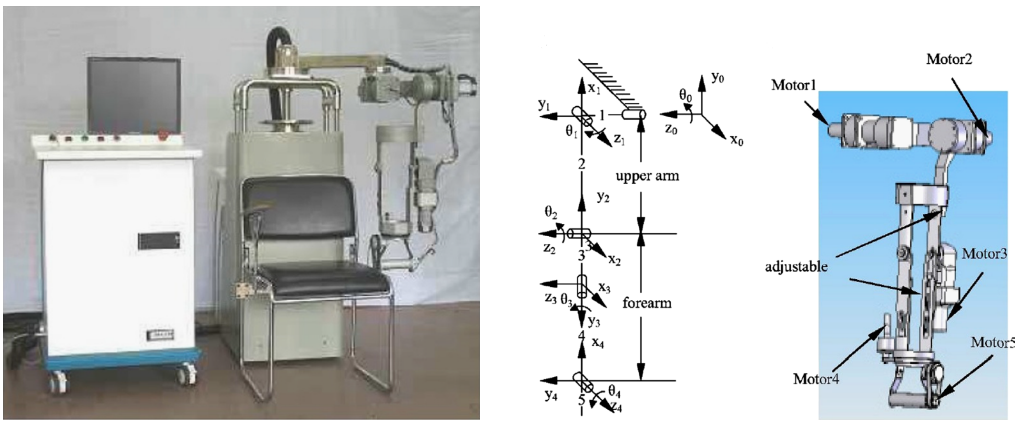

(A) Real View (B) Schematic View

FIGURE 1. Structure of the exoskeleton robot [11, 25]

TABLE 1. Items of the Dynamic Model

Symbol	Description	Size
θ	Angular position	(5x1)
$\dot{\theta}$	Angular velocity	(5x1)
$\ddot{\theta}$	Angular acceleration	(5x1)
$D(\theta)$	Inertia matrix	(5x5)
$H(\theta, \dot{\theta})$	Centrifugal and Coriolis matrix	(5x5)
$G(\theta)$	Gravitational vector	(5x1)
τ_{dis}	Disturbance vector	(5x1)
τ	Torque vector	(5x1)

2.2. Modeling of the system

In accordance with the schematic diagram of the robot depicted in Figure.1b, the mathematical dynamic model for the five-degrees-of-freedom exoskeleton robot is obtained using the Lagrange formalism of rigid bodies [26]. It is expressed in (1):

$$D(\theta)\ddot{\theta} + H(\theta, \dot{\theta})\dot{\theta} + G(\theta) + \tau_{dis} = \tau \tag{1}$$

Table. 1 summarizes the description of elements of the dynamic model of the five-degrees-of-freedom exoskeleton robot in (1).

$$\begin{aligned} D(\theta) &= D_n(\theta) + \Lambda D(\theta) \\ H(\theta, \dot{\theta}) &= H_n(\theta, \dot{\theta}) + \Lambda H(\theta, \dot{\theta}) \\ G(\theta) &= G_n(\theta) + \Lambda G(\theta) \end{aligned} \tag{2}$$

where $D_n(\theta)$, $H_n(\theta, \dot{\theta})$ and $G_n(\theta)$ denote nominal terms and $\Lambda D(\theta)$, $\Lambda H(\theta, \dot{\theta})$ and $\Lambda G(\theta)$ denote parametric uncertainties.

In [11, 25], the complete definition and different entries of the matrices constituting (1) of the exoskeleton robot as well uncertainties and inertial characteristics are detailed. This description is too long, for convenience, it is not presented in this work.

The dynamic model is developed by combining the equations of (1) and (2) as:

$$D_n(\theta)\ddot{\theta} + H_n(\theta, \dot{\theta})\dot{\theta} + G_n(\theta) = \tau + \zeta(t) \tag{3}$$

$\zeta(t)$ is defined in (4) as a term that collects parametric uncertainties and disturbances assumed bounded.

$$\zeta(t) = -\Lambda D(\theta)\ddot{\theta} - \Lambda H(\theta, \dot{\theta})\dot{\theta} - \Lambda G(\theta) - \tau_{dis} \tag{4}$$

Taking advantage of invertibility of inertia matrix, (3) and (4) are rewritten in state space representation with state variables $z_1 = \theta$ and $z_2 = \dot{\theta}$ and $\nu = \tau$ gives:

$$\begin{cases} \dot{z}_1 = z_2 \\ \dot{z}_2 = f(z_1, z_2, t) + g(z_1)\,\nu \end{cases} \tag{5}$$

whereby $f(z_1, z_2, t)$ and $g(z_1)$ are defined in (6)

$$\begin{cases} f(z_1, z_2, t) = {D_n}^{-1}(z_1)(-H_n(z_1, z_2) - G_n(z_1) + \zeta(t)) \\ g(z_1) = D_n^{-1}(z_1) \end{cases} \tag{6}$$

Equation (7) defines ν as:

$$\nu = g^{-1}(z_1)\,u \tag{7}$$

Finally, the closed loop perturbed and coupled system of the exoskeleton robot to be controlled is then presented as:

$$\begin{cases} \dot{z}_1 = z_2 \\ \dot{z}_2 = u + f(z_1, z_2, t) \end{cases} \tag{8}$$

Remark: The notation $\lfloor . \rceil^r = |.|^r \operatorname{sign}(.)$, is used in the sequel to simplify expressions, $r \in \mathbb{R}$. For example:

$$\lfloor . \rceil^0 = \operatorname{sign}(.), \quad \lfloor . \rceil^0 . ^r = |.|^r, \quad \lfloor . \rceil^0 |.|^r = \lfloor . \rceil^r$$

3. Controller Design

A robust finite-time saturated control strategy will be investigated in this section to track desired trajectories of a five-degrees-of-freedom exoskeleton robot. Further, the saturated controller protects electrical actuators and expends their life-time.

3.1. Control objective

As to address the trajectory tracking control task applied to the upper limb exoskeleton robot, torques of joints are designed in such a way that the joint's positions θ reach the desired trajectories θ_d in finite-time. These latter are considered twice differentiable. Therefore, the angular position tracking error vector is given by $e_1 = \theta - \theta_d$ while its time derivative is expressed by $e_2 = \dot{\theta} - \dot{\theta}_d$. Consequently, the closed loop error dynamics model is expressed in (9).

$$\begin{cases} \dot{e}_1 = e_2 \\ \dot{e}_2 = u + f(z_1, z_2, t) - \ddot{\theta}_d \end{cases} \tag{9}$$

By referring to (9), the tracking objective can be defined as $\lim_{t \to T} e_1 = 0$, and $e_1 = 0$ for t $\geq$ T wherein T is the finite convergence time.

3.2. Saturated Finite-time SMC algorithm

A saturated robust control scheme based on the 3-STA controller [19] will be developed to control the five-degree-of-freedom exoskeleton robot based on the previous system definition (9) to achieve (10). This controller takes the maximum torques limits of the actuators in account to preserve them.

Theorem 1. The saturated control law defined by:

$$u = sat\left(-\alpha_1 \lfloor \psi \rceil^{\frac{1}{2}} + L\right) \tag{10}$$

$$\dot{L} = \begin{cases} -\alpha_3 \lfloor \psi \rceil^0 & if \quad |u| \leq U \\ 0 & if \quad |u| > U \end{cases} \tag{11}$$

with initial state $L(0) = 0$ and sat is saturation function with maximum amplitude U.

Gains $\alpha_1, \alpha_2, \alpha_3$ are positive and $\psi = e_2 + \alpha_2 \lfloor e_1 \rceil^{\frac{2}{3}}$. This controller establishes finite-time convergence for any Lipschitz disturbance $f(z_1, z_2, t)$. It follows that, the tracking error converges to the origin after a finite transient time. That is $e_1 = e_2 = \dot{e}_2 = 0$ for all $t > t_r$ with t_r reaching time and the control u remains bounded $\forall t > 0$

The saturation function sat is defined as:

$$sat(y) = \begin{cases} y & ||y|| \leq M \\ M \lfloor y \rceil^0 & ||y|| > M \end{cases} \tag{12}$$

Proof:

The saturated controller in (10) and (11) is essentially designed to prevent exceeding the maximum torques of the electrical motors driving the joints of the exoskeleton robot. The stability proof is considered for the two domains according to the magnitude of the control signal.

First : for $|u| \leq U$ **,** the expression of the controller is given by u_1

$$u_1 = -\alpha_1 \lfloor \psi \rceil^{\frac{1}{2}} + \int_0^t -\alpha_3 \lfloor \psi \rceil^0 \tag{13}$$

This controller is proposed in [19] as a third order super twisting algorithm (3-STA) with finite-time convergence.

Subsequently, the closed loop system (9) with controller (13) is written as:

$$\begin{cases} \dot{e}_1 = e_2 \\ \dot{e}_2 = -\alpha_1 \lfloor \psi \rceil^{\frac{1}{2}} - \alpha_3 \int_0^t \lfloor \psi \rceil^0 dt + f(z_1, z_2, t) - \ddot{\theta}_d \end{cases} \tag{14}$$

Setting $e_3 = -\alpha_3 \int_0^t \lfloor \psi \rceil^0 + f(z_1, z_2, t) - \ddot{\theta}_d$

$$\begin{cases} \dot{e}_1 = e_2 \\ \dot{e}_2 = -\alpha_1 \lfloor \psi \rceil^{\frac{1}{2}} + e_3 \\ \dot{e}_3 = -\alpha_3 \lfloor \psi \rceil^{0} + \dot{f}\left(z_1, z_2, t\right) \end{cases} \tag{15}$$

The system in (15) is homogeneous [27], with a negative degree of $d = -1$ and weights of $r = [3\ 2\ 1]$. This algorithm coincides with the class of second order sliding mode controllers, in which only configuration variables z_1 and z_2 are needed to stabilize the system's states e_1, e_2 and e_3 in finite-time using a continuous input control signal. To cancel out the disturbances, an additional discontinuous integral term is added.

The proof of stability of (13) and the necessary conditions for the gains of the controller are detailed in [19]. Using vector $\Xi = \left[\lfloor e_1 \rceil^{\frac{2}{3}} \psi \left\lfloor \lfloor e_3 \rceil^{2} \right] \right.$, the Lyapunov function (16) is proposed in quadratic form.

$$V = \Xi^T W \Xi \text{ , with } W = \begin{bmatrix} w_1 & -\frac{1}{2}w_{12} & \frac{1}{2}w_{13} \\ -\frac{1}{2}w_{12} & w_2 & -\frac{1}{2}w_{23} \\ \frac{1}{2}w_{13} & -\frac{1}{2}w_{23} & w_3 \end{bmatrix} \tag{16}$$

The aim is to develop conditions for coefficients $(w_1, w_{12}, w_2, w_{13}, w_{23}, w_3)$ and gains α_1, α_2 and α_3 such that $V > 0$ and $\dot{V}$ along trajectories of (9) is negative definite.

$$\begin{aligned} V = {} & w_1 \left|e_1\right|^{\frac{4}{3}} - w_{12} \lfloor e_1 \rceil^{\frac{2}{3}} \psi + w_2 \left|\psi\right|^2 \\ & + w_{13} \lfloor e_1 \rceil^{\frac{2}{3}} \lfloor e_3 \rceil^2 - w_{23} \psi \lfloor e_3 \rceil^2 + w_3 \left|e_3\right|^4 \end{aligned} \tag{17}$$

This Lyapunov function is in (17) homogeneous of degree 4 with weights [3 2 1].

Consider conditions on coefficients (16):

$$\begin{aligned} & w_1 > 0 \\ & w_1 w_2 > \tfrac{1}{4} w_{12}^2 \\ & w_1 \left(w_2 w_3 - w_{23}^2\right) + \tfrac{w_{12}}{2} \left(-\tfrac{w_{12} w_3}{2} + \tfrac{w_{13} w_{23}}{4}\right) \\ & + \tfrac{w_{13}}{2} \left(\tfrac{w_{12} w_{23}}{4} - \tfrac{w_2 w_{13}}{2}\right) > 0 \end{aligned} \tag{18}$$

Based on the theorem in [19], it is stated that if (16) are satisfied for Lyapunov function (16), then $\dot{V}$ meets the differential inequalities

$$\dot{V} \leq -\kappa V^{3/4} \tag{19}$$

for some positive κ if gains α_1, α_2 and α_3 are appropriately designed. The proof of this statement is provided in [19].

Second : for $|u| > U$ **,** in this case the control law is outside the bounds and is regulated by the following controller:

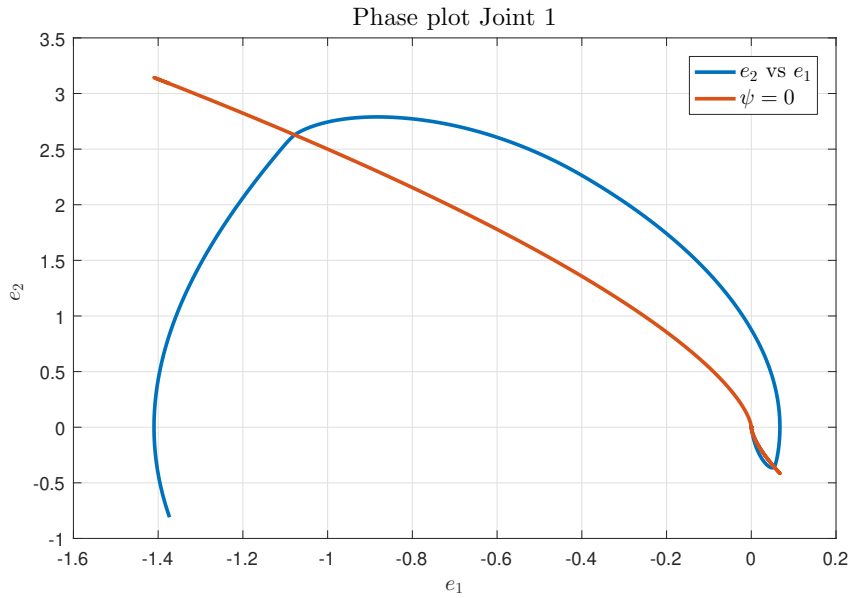

FIGURE 2. Phase plot for joint 1

$$u_2 = U \left\lfloor -\alpha_1 \lfloor \psi \rceil^{\frac{1}{2}} \right\rceil^0 \tag{20}$$

which can be expanded as

$$u_2 = U \left\lfloor -\alpha_1 \left\lfloor e_2 + \alpha_2 \lfloor e_1 \rceil^{\frac{2}{3}} \right\rceil^{\frac{1}{2}} \right\rceil^0 \tag{21}$$

This controller has the form of a second order sliding mode with prescribed convergence [28, 29].The nonlinear sliding manifold is $e_2 + \alpha_2 \lfloor e_1 \rceil^{\frac{2}{3}}$. The system trajectories of the exoskeleton robot (9) reach this sliding surface before switching the 3-STA control. Usually, the torques inputs at start are high, this insures having second-order behavior of sliding modes while saturating them.

The e_1, e_2 plane is divided into two sections by the manifold ψ (see Figure. 2). The sliding manifold is attractive. The origin, i.e.$(e_1, e_2 = 0)$ is reached in finite-time. It can be observed that a super-twisting like phase evolution happens.

The closed loop system becomes using (20) is given by:

$$\begin{cases} \dot{e}_1 = e_2 \\ \dot{e}_2 = U \left\lfloor -\alpha_1 \left\lfloor e_2 + k_2 \lfloor e_1 \rceil^{\frac{2}{3}} \right\rceil^{\frac{1}{2}} \right\rceil^0 + f\left(z_1, z_2, t\right) - \ddot{\theta}_d \end{cases} \tag{22}$$

TABLE 2. Exoskeleton robot motor specifications [23]

	Output torque (N.m)	Output speed (rpm)	Type of Motor	Range of Motion (rad)
Shoulder Joint 1	46	3.75	RE40-148867	$-\pi/4$ ~ $\pi/2$
Shoulder Joint 2	46	3.75	RE40-148867	0 ~ $\pi/2$
Elbow Joint 3	27.96	4.76	RE40-148867	0 ~ 0.694π
Rotation Joint 4	3.24	4.76	Amax26-110963	$-\pi/2$ ~ $\pi/2$
Wrist Joint 5	0.620	33	Remax17-215996	$-\pi/4$ ~ 0.416π

4. **Numerical Simulations**

This section discusses the results of numerical simulation of the trajectory tracking control task issued from the application of the proposed saturated finite-time third order sliding mode controller to the five-degrees-of-freedom upper limb exoskeleton robot. This controller will be compared to the 3-STA controller in [19] under the same conditions.

The specification about choice of motors of the five-degrees-of-freedom exoskeleton robot of Figure. 1 are stated in Table. 2 [23]. The saturated control is designed to respect these motor specifications for each joint of the exoskeleton robot.

4.**1**. **Methodology**

At first, the full dynamic model of the exoskeleton robot (9) is implemented in Matlab/Simulink. Information on the inertial constants of the robot and the gravitational constants are provided in [11] as well as the uncertainties affecting these physical elements.

The joint's initial positions and velocities are selected as:
$\theta(0) = \left[\frac{-\pi}{4}\ \frac{\pi}{5}\ \frac{-\pi}{6}\ \frac{-\pi}{4}\ \frac{\pi}{5}\right]^T$ and $\dot{\theta}(0) = [0\ 0\ 0\ 0\ 0]^T$ respectively.

Whereas the desired trajectories are defined by:

$$\theta_{d_j} = \left(sin\left(t + n.\frac{\pi}{5}\right)\right) \tag{23}$$

where $j = 0..5$ the joints number and $n = n + 1; \quad n(0) = 0$

The time-varying permanent disturbance vector τ_{dis} is considered in (24). It is as well depicted in Figure. 3 .

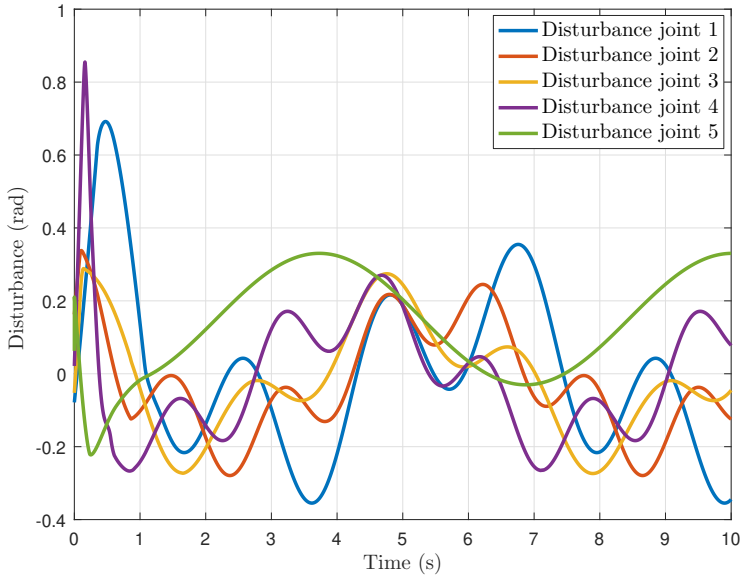

FIGURE 3. Disturbance signals applied to the joints of the exoskeleton robot

$$\boldsymbol{\tau}_{dis} = 0.15\ \dot{\theta} + 0.1\ \theta + [0.2\sin(3t) \quad 0.1\cos(4t) \quad 0.1\sin(3t) \quad 0.1\cos(4t) \quad 0.15\sin(4t)]^T \tag{24}$$

Due to the large number of nonlinear inequalities that must be satisfied and the fact that the exoskeleton system's model is very nonlinear and coupled, it is very difficult to find a set of gains and parameters that satisfy all of the necessary conditions using the proposed Lyapunov functions. As a result, the gains are adjusted throughout simulations to get the best performance in trajectory tracking. Table. 3 lists the employed gains.

TABLE 3. Parameters of the controllers

	3-STA	Saturated SSTA
α_1	[5.5 10.5 20.5 20.5 10.5]	[10.5 20.5 30.5 35.5 10.5]
α_2	[1.7 1.7 1.7 5.5 1.7]	[2.5 2.1 2.0 7.5 2.7]
α_3	[10.2 10.2 20.2 5.2 10.2]	[10.2 10.2 20.2 25.2 10.2]

4.2. Analysis of obtained results

To analyse the efficiency of the proposed algorithms in achieving the trajectory tracking control task, we will first consider the position output of the five joints of the exoskeleton robot. Results of trajectory tracking results are illustrated in Figure. 4 and Figure. 5.

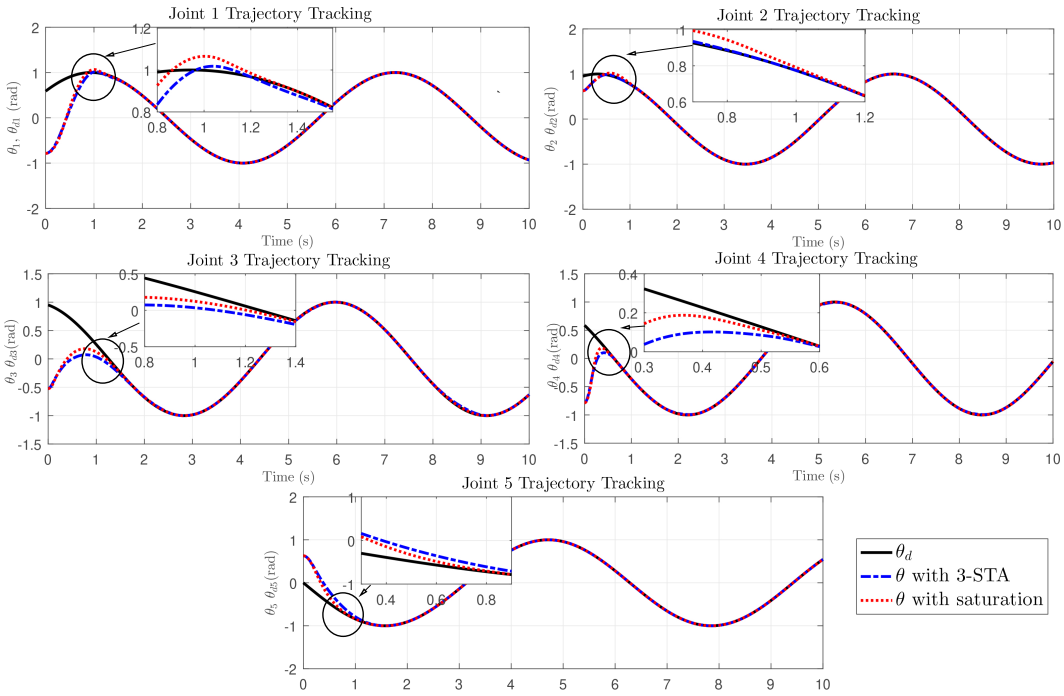

FIGURE 4. Exoskeleton robot trajectory tracking results

It is observed from Figure. 4 that tracking is successfully achieved using both controllers in finite-time. However, it can be viewed from the zoom that the saturated finite-time SMC controller behaves slightly better as it converges faster for all joints without overshoot except for the second joint. This is confirmed in the trajectory tracking errors plot Figure. 5. This can be attributed to the coupling and non-linearity of the dynamic model and the saturation bounds.

Figure. 6 shows the control signals of the saturated and the unsaturated finite-time SMC controllers. Saturation bounds are depicted as well. It should be noted that disturbances and uncertainties are time varying, state-dependent and non-vanishing. The control inputs are continuous signals.

Therefore, it is noticed from Figure. 6 that when applying the unsaturated controller, the maximum torque input to each joint of the exoskeleton robot exceeds the saturation limits presented by dashed lines on the plots. In contrast, the saturated control inputs are always within the saturation limits defined by the physical constraints on the associated motor to each joint of the exoskeleton robot without altering the tracking precision. It can also be viewed, that for the elbow joint 3, both controllers respect the saturation conditions. This can be confirmed from Figure. 7 (right).

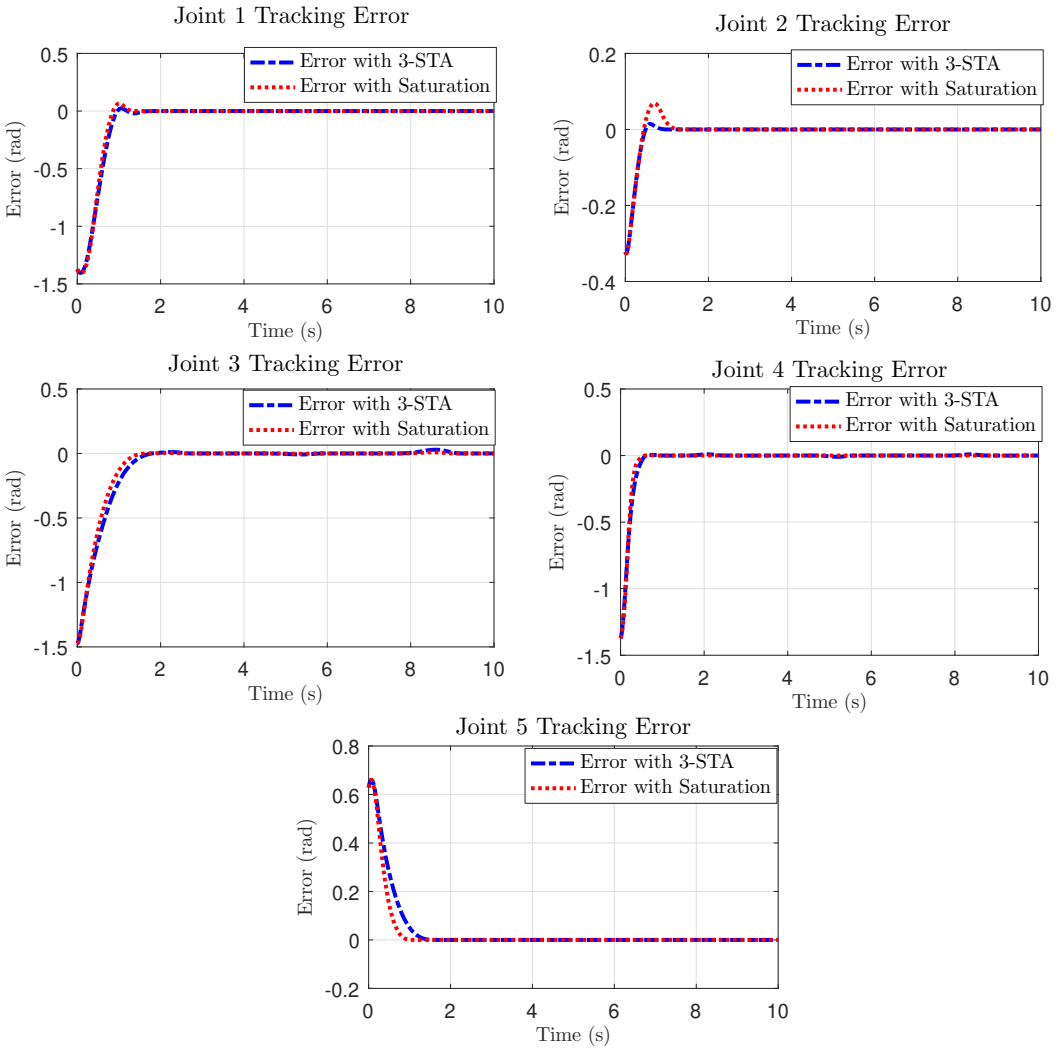

FIGURE 5. Tracking error curves for the exoskeleton robot joints

It is reported in Figure. 7 metrics to evaluate the precision of the two controllers to be compared. To the left, the plot of the root-mean square tracking errors (RMSE) are displayed for each joint. It indicates the best fit to the desired trajectory. The smaller the RMSE the closer the output to the desired one. It is calculated using the following formula:

$$\mathrm{err_i} = \left[\sum_{t=0}^{N.\varpi} \left(\theta_i(t) - \theta_{id}(t)\right)^2 / N \right]^{1/2} \tag{25}$$

with $i = 1..5$ is the joint's number, N is the sample's number and $\varpi = 0.001s$ is the sampling period.

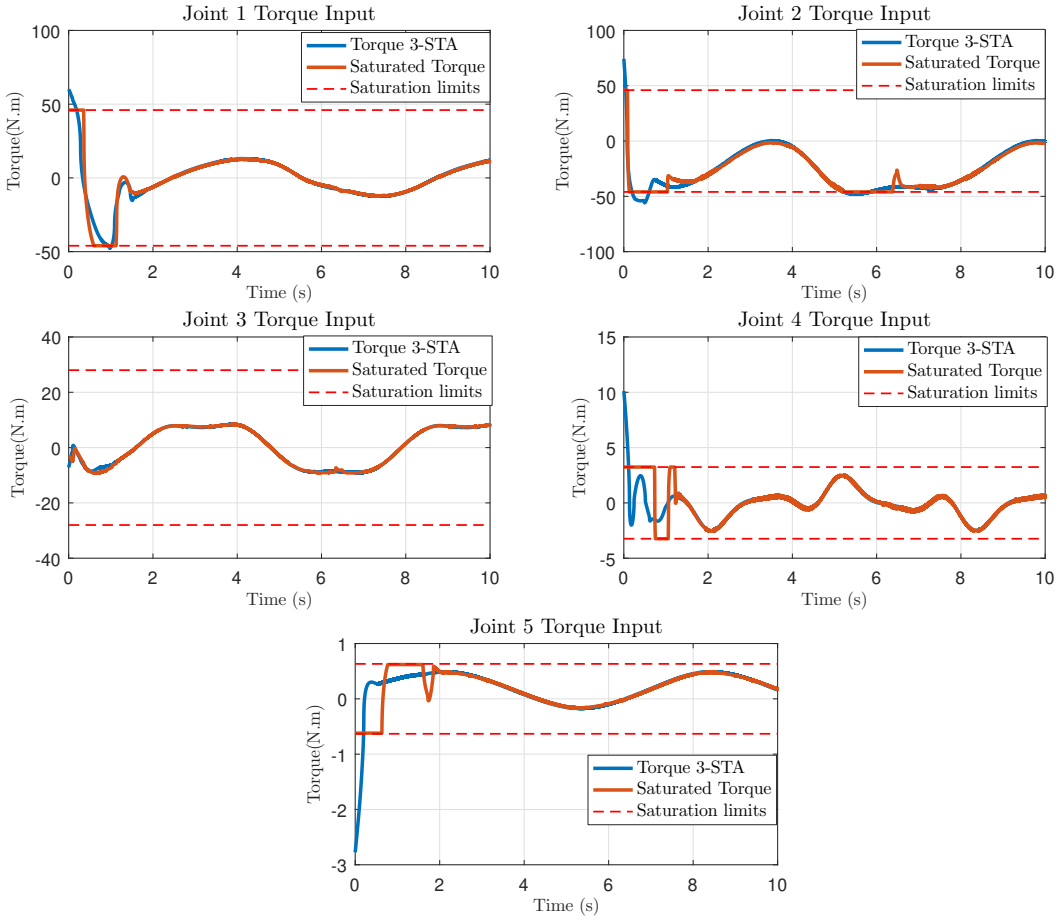

FIGURE 6. Control input torques applied to the exoskeleton robot

From the bar plot, it is noticed that the precision of the two controllers is good with slight advantage to the saturated control. On the other hand, it is quite clear from the bar plot of the maximum absolute input torques Figure. 7 that the saturated controller delivers less energy to the exoskeleton robot's actuators. It can be noticed that two first joints of the exoskeleton robot related to shoulder movements are associated to more powerful motors.

In theory, by increasing the order of the controller, the precision obtained in the sliding surface increases, but in turn, the complexity of the control law and the consumption of computational resources increases. On the other hand, in practice, the maximum achievable precision is restricted by the presence of limitations on the physical constraints on actuators which should be taken into account. These limitations usually that do not allow the properties of sliding modes to be exploited to the maximum. Throughout this work, a

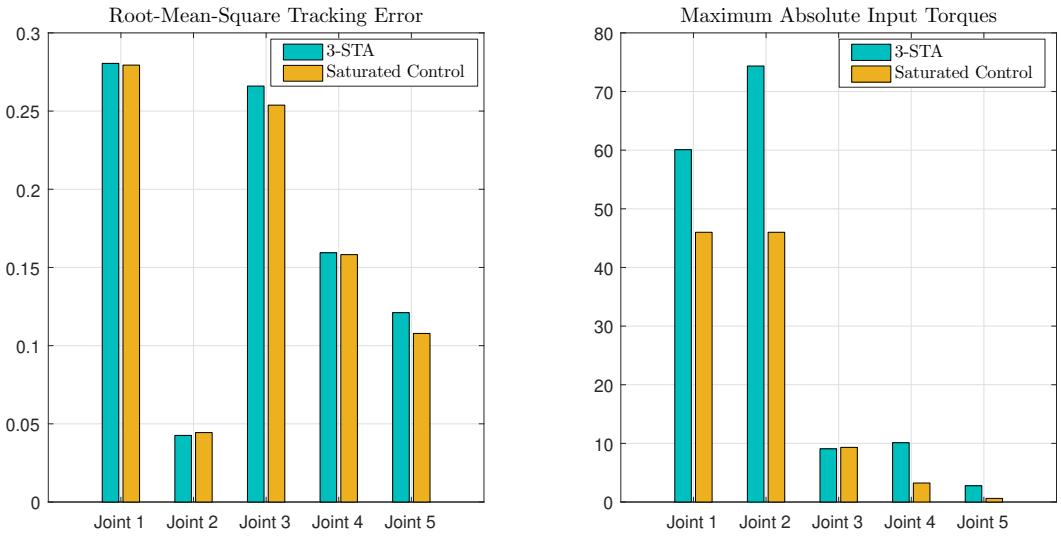

FIGURE 7. Root-mean square of tracking error (left) and maximum energy comparison (right)

saturated finite-time higher order sliding mode controller founded on the third-order homogeneous super-twisting controller achieved trajectory tracking task efficiently by compensating for certain types of disturbances with a finite-time convergence and an increase in the precision.

5. Conclusion

In the present work, a new saturated finite-time higher-order sliding mode control algorithm was examined for the first time to control a five-degrees-of-freedom upper limb exoskeleton robot, obtaining highly satisfactory results. Trajectory tracking control objective of the position of the joints of the exoskeleton robot under the proposed controllers was carried out with a good performance and faster finite-time convergence. The saturated controller's produces continuous control system which alleviates the chattering problem and compensates for disturbances and uncertainties. Furthermore, it takes into account the physical limitations on actuators of the exoskeleton robot and thus delivers a bounded input torque sufficient enough to achieve the control task while preserving life-time of the actuators. Numerical simulation results are presented to demonstrate the efficacy of the proposed approach. In order to avoid overestimation of the gains of the controller and the necessity to have prior knowledge about bounds of uncertainties, our future research will focus on the proposition of adaptation laws, as well as an experimental evaluation of the proposed control strategies.

REFERENCES

[1] N. Rehmat, J. Zuo, W. Meng, Q. Liu, S. Q. Xie, and H. Liang, "Upper limb rehabilitation using robotic exoskeleton systems: a systematic review," *International Journal of Intelligent Robotics and Applications*, vol. 2, no. 3, pp. 283–295, 2018.

[2] A. Demofonti, G. Carpino, L. Zollo, and M. J. Johnson, "Affordable robotics for upper limb stroke rehabilitation in developing countries: a systematic review," *IEEE Transactions on Medical Robotics and Bionics*, pp. 1–1, 2021.

[3] I. Büsching, A. Sehle, J. Stürner, and J. Liepert, "Using an upper extremity exoskeleton for semi-autonomous exercise during inpatient neurological rehabilitation-a pilot study," *Journal of neuroengineering and rehabilitation*, vol. 15, no. 1, pp. 1–7, 2018.

[4] Q. Miao, M. Zhang, J. Cao, and S. Q. Xie, "Reviewing high-level control techniques on robot-assisted upper-limb rehabilitation," *Advanced Robotics*, vol. 32, no. 24, pp. 1253–1268, 2018.

[5] J.-J. E. Slotine, W. Li, *et al.*, *Applied nonlinear control*, vol. 199. prentice-Hall Englewood Cliffs, NJ, 1991.

[6] R. Fellag, T. Benyahia, M. Drias, M. Guiatni, and M. Hamerlain, "Sliding mode control of a 5 dofs upper limb exoskeleton robot," in *2017 5th International Conference on Electrical Engineering - Boumerdes (ICEE-B)*, pp. 1–6, Oct 2017.

[7] M. H. Rahman, M. Saad, J.-P. Kenné, and P. S. Archambault, "Control of an exoskeleton robot arm with sliding mode exponential reaching law," *International Journal of Control, Automation and Systems*, vol. 11, pp. 92–104, jan 2013.

[8] T. Madani, B. Daachi, and K. Djouani, "Non-singular terminal sliding mode controller: Application to an actuated exoskeleton," *Mechatronics*, vol. 33, pp. 136–145, 2016.

[9] R. Fellag, M. Hamerlain, S. Laghrouche, M. Guiatni, and N. Achour, "Homogeneous finite time higher order sliding mode control applied to an upper limb exoskeleton robot," in *2019 6th International Conference on Control, Decision and Information Technologies (CoDIT)*, pp. 355–360, 2019.

[10] X. Wang, X. Li, J. Wang, X. Fang, and X. Zhu, "Data-driven model-free adaptive sliding mode control for the multi degree-of-freedom robotic exoskeleton," *Information Sciences*, vol. 327, pp. 246–257, 2016.

[11] H.-B. Kang and J.-H. Wang, "Adaptive control of 5 dof upper-limb exoskeleton robot with improved safety," *ISA transactions*, vol. 52, no. 6, pp. 844–852, 2013.

[12] A. Riani, T. Madani, A. Benallegue, and K. Djouani, "Adaptive integral terminal sliding mode control for upper-limb rehabilitation exoskeleton," *Control Engineering Practice*, vol. 75, pp. 108–117, 2018.

[13] A. Jebri, T. Madani, and K. Djouani, "Adaptive continuous integral-sliding-mode controller for wearable robots: Application to an upper limb exoskeleton," in *2019 IEEE 16th International Conference on Rehabilitation Robotics (ICORR)*, pp. 766–771, IEEE, 2019.

[14] I. Castillo, M. Steinberger, L. Fridman, J. A. Moreno, and M. Horn, "A lyapunov based saturated super-twisting algorithm," in *Emerging Trends in Sliding Mode Control*, pp. 47–68, Springer, 2021.

[15] M. A. Golkani, S. Koch, M. Reichhartinger, and M. Horn, "A novel saturated super-twisting algorithm," *Systems & Control Letters*, vol. 119, pp. 52–56, 2018.

[16] I. Castillo, M. Steinberger, L. Fridman, J. Moreno, and M. Horn, "Saturated super-twisting algorithm based on perturbation estimator," in *2016 IEEE 55th Conference on Decision and Control (CDC)*, pp. 7325–7328, IEEE, 2016.

[17] R. Seeber and M. Horn, "Guaranteeing disturbance rejection and control signal continuity for the saturated super-twisting algorithm," *IEEE Control Systems Letters*, vol. 3, no. 3, pp. 715–720, 2019.

[18] M. A. Golkani, R. Seeber, M. Reichhartinger, and M. Horn, "Lyapunov-based saturated continuous twisting algorithm," *International Journal of Robust and Nonlinear Control*, 2020.

[19] S. Kamal, A. Chalanga, J. A. Moreno, L. Fridman, and B. Bandyopadhyay, "Higher order super-twisting algorithm," in *2014 13th International Workshop on Variable Structure Systems (VSS)*, pp. 1–5, IEEE, 2014.

[20] P. Yang, X. Ma, J. Wang, G. Zhang, Y. Zhang, and L. Chen, "Disturbance observer-based terminal sliding mode control of a 5-dof upper-limb exoskeleton robot," *IEEE Access*, vol. 7, pp. 62833–62839, 2019.

[21] A. Abooee, M. M. Arefi, F. Sedghi, and V. Abootalebi, "Robust nonlinear control schemes for finite-time tracking objective of a 5-dof robotic exoskeleton," *International Journal of Control*, pp. 1–16, 2018.

[22] B. O. Mushage, J. C. Chedjou, and K. Kyamakya, "Fuzzy neural network and observer-based fault-tolerant adaptive nonlinear control of uncertain 5-dof upper-limb exoskeleton robot for passive rehabilitation," *Nonlinear Dynamics*, vol. 87, no. 3, pp. 2021–2037, 2017.

[23] Q. Li, D. Wang, Z. Du, and L. Sun, "A novel rehabilitation system for upper limbs," in *2005 IEEE Engineering in Medicine and Biology 27th Annual Conference*, pp. 6840–6843, IEEE, 2006.

[24] J. Wang, Z. Jiang, X. Wang, Y. Zhang, and D. Guo, "Kinematics simulation of upper limb rehabilitant robot based on virtual reality techniques," in *2011 2nd International Conference on Artificial Intelligence, Management Science and Electronic Commerce (AIMSEC)*, pp. 6681–6683, IEEE, 2011.

[25] H.-B. Kang and J.-H. Wang, "Adaptive robust control of 5 dof upper-limb exoskeleton robot," *International Journal of Control, Automation and Systems*, vol. 13, no. 3, pp. 733–741, 2015.

[26] M. W. Spong and M. Vidyasagar, *Robot dynamics and control*. John Wiley & Sons, 2008.

[27] A. Levant, "Homogeneity approach to high-order sliding mode design," *Automatica*, vol. 41, no. 5, pp. 823–830, 2005.

[28] A. Levant, "Sliding order and sliding accuracy in sliding mode control," *International journal of control*, vol. 58, no. 6, pp. 1247–1263, 1993.

[29] Y. Shtessel, C. Edwards, L. Fridman, and A. Levant, *Sliding mode control and observation*, vol. 10. Springer, 2014.